PROCEEDINGS OF SCIENCE

Latest Muon Neutrino Disappearance Results from IceCube DeepCore

Anil Kumar[a,*] **for the IceCube collaboration**[*]

[a] *Deutsches Elektronen-Synchrotron DESY,*
Platanenallee 6, 15738 Zeuthen, Germany

E-mail: anil.kumar@desy.de

The IceCube Neutrino Observatory at the South Pole is a Cherenkov-based detector inside antarctic ice with a volume of about 1 cubic kilometer. IceCube consists of 5160 Digital Optical Modules (DOMs) attached like beads on 86 vertical strings, instrumenting depths from 1450 - 2450 m below the surface of the glacier. The bottom central region of IceCube has densely spaced DOMs and is known as DeepCore, which is capable of detecting atmospheric neutrinos at GeV energies. Atmospheric neutrinos can be used to study neutrino oscillations over wide ranges of energies and baselines. We present a measurement of the oscillation parameters Δm^2_{32} and θ_{23} using the disappearance of atmospheric muon neutrinos with a new data sample from IceCube DeepCore. This sample consists of improved data calibration, detector simulation, and data processing, as well as a more sophisticated treatment of systematics. These results are of comparative precision to measurements from long-baseline neutrino oscillation experiments.

**** The European Physical Society Conference on High Energy Physics (EPS-HEP 2023), ****
**** 21-25 August 2023 ****
**** Hamburg, Germany ****

[*] http://icecube.wisc.edu
[*] Speaker

© Copyright owned by the author(s) under the terms of the Creative Commons Attribution-NonCommercial-NoDerivatives 4.0 International License (CC BY-NC-ND 4.0).

PoS(EPS-HEP2023)179

1. Introduction

The phenomenon of neutrino-flavor oscillations has been observed and validated at various experiments using neutrinos from sources such as the atmosphere, accelerators, sun, and nuclear reactors. Neutrino oscillations can be explained by representing neutrino flavor eigenstates (ν_e, ν_μ, ν_τ) as a superposition of their mass eigenstates (ν_1, ν_2, ν_3). The neutrino mixing matrix can be parameterized in terms of three mixing angles (θ_{12}, θ_{13}, and θ_{23}), and one CP-phase (δ_{CP}). The neutrino oscillation probabilities also depend upon the mass-squared differences Δm^2_{21} and Δm^2_{32}. Out of these six oscillation parameters, θ_{12}, θ_{13}, and Δm^2_{21} have been measured with precisions of a few percent, whereas δ_{CP} and θ_{23} still have large uncertainties [1]. The magnitude of Δm^2_{32} is measured with a precision of a few percent; however, the sign is still unknown. The disappearance of atmospheric ν_μ at IceCube Neutrino Observatory can be used to measure θ_{23} and Δm^2_{32} [2]. In the two-flavor approximation, the survival probability of ν_μ with energy E after traveling a path-length L, can be written as

$$P(\nu_\mu \to \nu_\mu) = 1 - \sin^2(2\theta_{23}) \sin^2 \frac{1.27\Delta m^2_{32}[\mathrm{eV}^2]L[\mathrm{km}]}{E[\mathrm{GeV}]} \,. \tag{1}$$

Here, θ_{23} controls the amplitude of the oscillation, and Δm^2_{32} governs the frequency of the oscillation. Note that the analyses presented in this work use the three-flavor oscillations of atmospheric neutrinos with matter effects considering the Preliminary Reference Earth Model (PREM) [3].

Atmospheric neutrinos are produced in cosmic ray air showers. These neutrinos, with energies from a few MeV to more than TeV, travel through Earth over a large range of baselines up to ~12,000 km in the upward direction before being detected. Therefore, IceCube exploits atmospheric neutrinos over a broad band of L/E to efficiently observe the ν_μ survival probability. In Fig. 1, the ν_μ survival probability is shown in the plane of neutrino energy and cosine zenith angle $\cos\theta_z$ (a proxy for baseline L). In this oscillogram, θ_{23} affects the depth (amplitude) of the oscillation valley (blue strips) while Δm^2_{32} decides the location (frequency) of the valley.

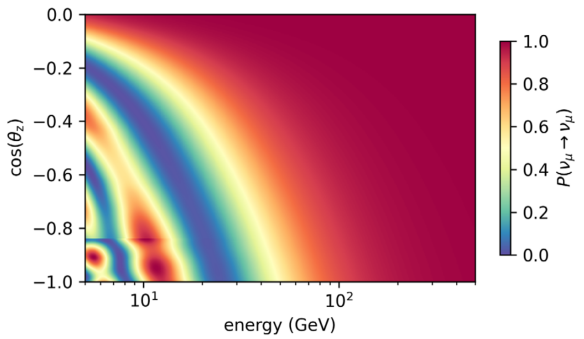

Figure 1: The ν_μ survival probability in the plane of energy and cosine zenith angle for upward-going neutrinos [2].

2. IceCube DeepCore Detector

The IceCube Neutrino Observatory [4] is located deep inside the antarctic ice at the South Pole. The interactions of neutrinos in the ice produce relativistic, secondary charged particles which emit

PoS(EPS-HEP2023)179

Cherenkov radiation. IceCube consists of 86 vertical strings with 60 Digital Optical Modules (DOMs) on each to detect these Cherenkov photons. IceCube is sensitive to neutrinos in the energy range of a few hundred GeV to a few PeV. The bottom central region of IceCube has more closely spaced DOMs and is known as DeepCore [4, 5], which extends the neutrino energy region down to approximately 5 GeV. The energy range of about 5 – 200 GeV enables DeepCore to efficiently observe the ν_μ disappearance signal shown in Fig. 1. This measurement is complementary to the relatively lower energy measurements at long-baseline experiments having different kinds of systematic uncertainties [6–8].

3. Reconstruction and Event Selection

The deep-inelastic charged-current (CC) interactions of ν_μ produce muons that travel long distances inside the detector and result in photon hits on DOMs in the form of track-like events as shown in the left panel of Fig 2. The τ leptons from ν_τ CC interactions decay to muons with a branching ratio of about 17% but any subsequent muon has a much lower energy than the original ν_τ and will be most often classified as a cascade due to the short track of muon. The ν_e CC (electromagnetic showers) and neutral-current (NC) interactions for all flavors (hadronic showers) give rise to photon hits on DOMs in the form of cascade-like events as shown in the middle panel of Fig 2. Cosmic muons and random noise from DOM are the main sources of background. The right panel of Fig. 2 shows data rates at various filter levels that reduce the cosmic muon and noise background below 1 percent of the neutrino signal [2]. After these filters, the background is low enough that the reconstruction algorithms can be applied on data to obtain observables like event energy, direction, and type of interaction, which are used in the oscillation analysis.

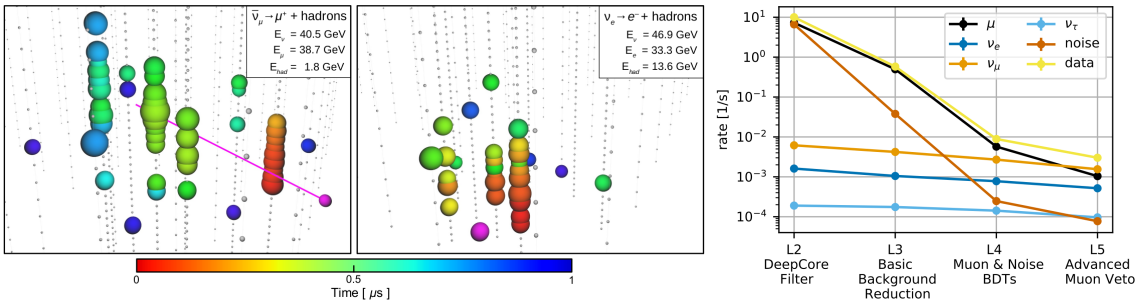

Figure 2: The left and middle panels correspond to track-like (ν_μ CC) and cascade-like (ν_e CC) events at DeepCore [9]. The right panel presents events rates after application of each filter [2].

3.1 Verification Sample

A subset of events called Verification sample (or golden event sample) is chosen to validate the new detector calibration and filtering, and ensure good agreement between data (recorded between 2011 - 2019) and simulation [2]. This sample consists of events with many direct, unscattered photons, and is optimized for ν_μ CC events. The direct photons allow an application of simple and fast reconstruction algorithms [10]. The SANTA algorithm is used to reconstruct the direction of neutrinos [10], whereas their energies are reconstructed using the LEERA algorithm [11]. A

PoS(EPS-HEP2023)179

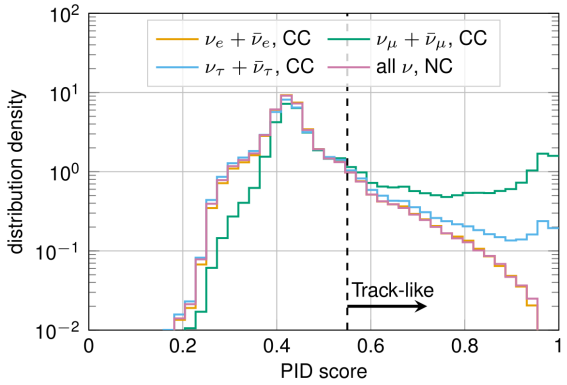

Figure 3: The PID score prediction by BDT output for various interaction types in the verification sample [2].

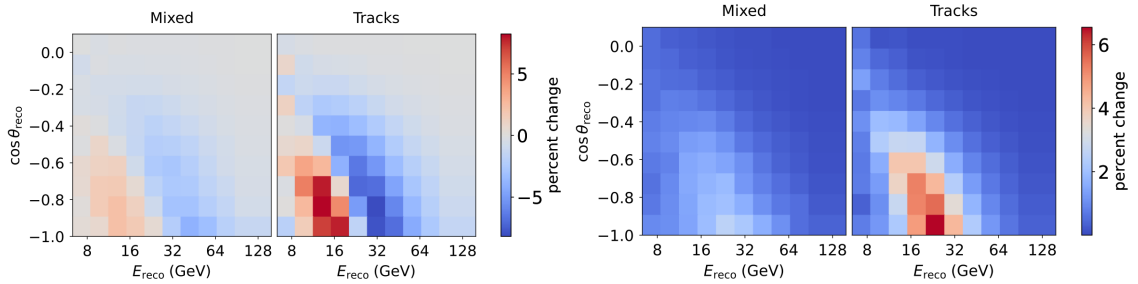

Figure 4: Effect of varying Δm^2_{32} (left) from 2.30×10^{-3} eV^2 to 2.55×10^{-3} eV^2 and $\sin^2\theta_{23}$ (right) from 0.43 to 0.58 on the expected event distributions for the verification sample [2].

Gradient Tree Boosting algorithm [12] is trained using the observables from these reconstructions and aims for the identification of track-like ν_μ CC events as signals against a background of cascade-like events. Figure 3 shows the particle identification (PID) score prediction by the boosted decision tree (BDT) algorithm for simulated events considering various interaction types. Events are classified into two bins: mixed ($0.55 < \text{PID} < 0.75$) and high-purity tracks ($0.75 < \text{PID} < 1$) corresponding to 70% and 94% ν_μ CC purity, respectively [2]. Figure 4 shows the modification in the expected event distribution on varying the values of Δm^2_{32} (left) and $\sin^2\theta_{23}$ (right) [2]. Here, Δm^2_{32} affects the positions of oscillation valleys and $\sin^2\theta_{23}$ governs the amplitudes of valleys.

3.2 CNN-reconstructed Sample

An algorithm based on convolutional neural networks (CNN) is used to reconstruct more complicated events (recorded between 2012-2021), including the ones with scattered photons [13–16]. For each DOM, the variables such as total charge, time of first charge, time of last charge, time-weighted mean of charges, and time-weighted standard deviations of charges are calculated from the digitized waveforms and are given as input to the CNN. Multiple CNNs are trained independently to reconstruct neutrino energy, arrival zenith angle, interaction vertex, PID, and a classifier for rejecting cosmic muon. Figure 5 shows the Monte Carlo (MC) distribution of PID predicted by CNN-reconstruction for different interaction types. Figure 6 presents the distribution of CNN-reconstructed simulated events as a function of reconstructed energy and cosine zenith angle of neutrinos for PIDs corresponding to cascade-, mixed-, and track-like topologies [13].

PoS(EPS-HEP2023)179

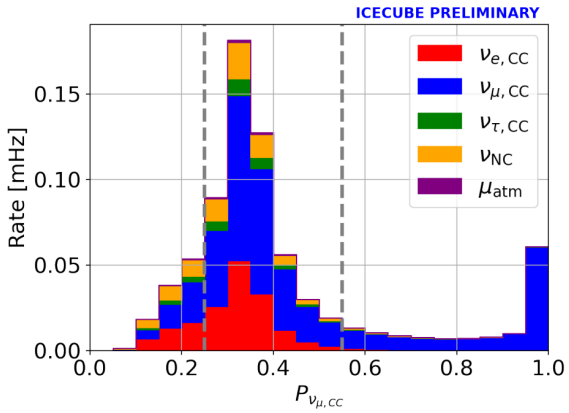

Figure 5: MC distribution of PID predicted by CNN for various interaction types (colored stacks) [13]. The dashed-vertical lines categorize events into cascades (left), mixed (middle), and tracks (right).

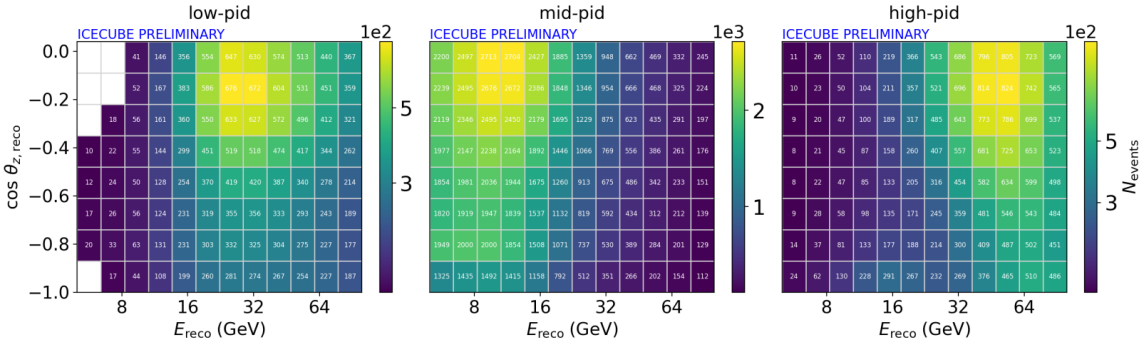

Figure 6: Distributions of CNN-reconstructed simulated events in the plane of reconstructed energy and cosine zenith angle of neutrinos for PIDs corresponding to cascade-, mixed-, and track-like topologies [13]. The white color corresponds to bins, which are not included in the analysis due to low MC statistics.

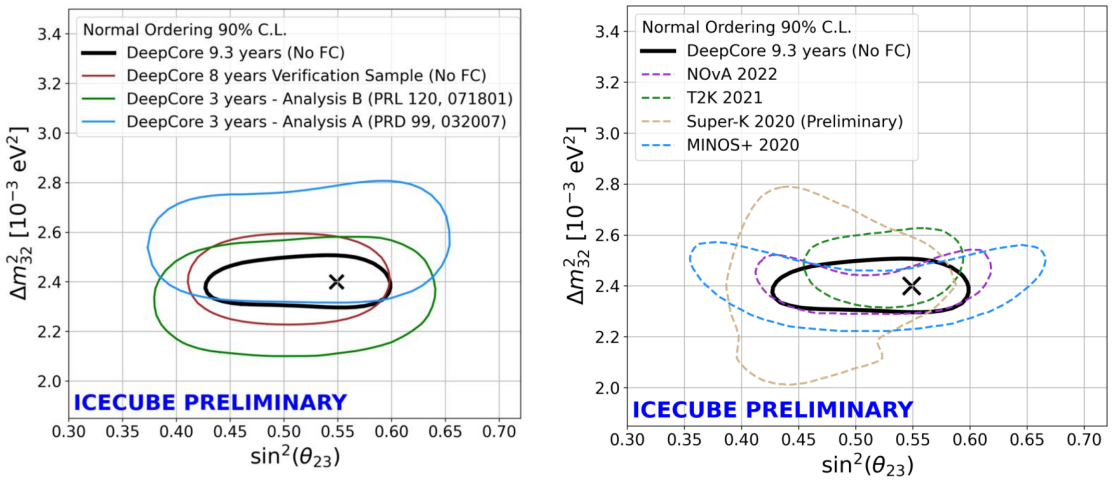

Figure 7: The confidence contours in the plane of $\sin^2\theta_{23}$ and Δm^2_{32} at 90% C.L. considering normal mass ordering [13]. The black and red contours assume Wilks theorem and have no Feldman-Cousins (No FC) corrections applied. The cross represents the best-fit point. The comparison with previous DeepCore results [17, 18] in the left panel and with other experiments [6–8, 19] in the right panel.

PoS(EPS-HEP2023)179

4. Results

The ν_μ disappearance analysis incorporates systematic errors for detector calibration uncertainties, atmospheric neutrino flux, cross-section, cosmic muons, and normalization as described in Ref. [2]. In Fig. 7, we show the contours (black and red) assuming Wilks' theorem (without Feldman-Cousins corrections) for the measurement of $\sin^2\theta_{23}$ and Δm^2_{32} at 90% C.L. considering normal mass ordering. In the left panel, we show a comparison among results of the CNN-based sample (black curve) [13], Verification sample (red curve) [2], and previous DeepCore results (green and blue curves) [17, 18]. In the right panel, we show the comparison of CNN-based DeepCore result (solid black curve) with results from other experiments (dashed-curves) [6–8, 19]. DeepCore results are competitive and complementary to that of long-baseline experiments. Since the current results are not systematically limited, further improvements are expected with DeepCore as data-taking continues, and new and improved reconstructions are developed. The measurement precision is expected to enhance significantly with the IceCube Upgrade detector, to be completed in early 2026, which will have more efficient DOMs, improved calibrations as well as the lower energy threshold of about a few GeV [20, 21].

References

[1] I. Esteban, M. C. Gonzalez-Garcia, M. Maltoni, T. Schwetz, A. Zhou, *JHEP* **09** (2020) 178.

[2] **IceCube** Collaboration, *Phys. Rev. D* **108** (2023), no. 1 012014.

[3] A. M. Dziewonski and D. L. Anderson, *Phys. Earth Planet. Interiors* **25** (1981) 297–356.

[4] **IceCube** Collaboration, *JINST* **12** (2017), no. 03 P03012.

[5] **IceCube** Collaboration, R. Abbasi et al., *Astropart. Phys.* **35** (2012) 615–624.

[6] **NOvA** Collaboration, *Phys. Rev. D* **106** (2022), no. 3 032004.

[7] **T2K** Collaboration, *Phys. Rev. D* **103** (2021), no. 11 112008.

[8] **MINOS+** Collaboration, *Phys. Rev. Lett.* **125** (2020), no. 13 131802.

[9] A. Terliuk, Ph.D. thesis, Humboldt-Universität zu Berlin, Mathematisch-Naturwissenschaftliche Fakultät I, 2018, DOI: 10.18452/19304.

[10] **IceCube** Collaboration, *Eur. Phys. J. C* **82** (2022), no. 9 807.

[11] **IceCube** Collaboration, *Phys. Rev. D* **91** (2015), no. 7 072004.

[12] J. H. Friedman, *Annals Statist.* **29** (2001), no. 5 1189–1232.

[13] **IceCube** Collaboration, *PoS* **ICRC2023** (2023) 1143.

[14] **IceCube** Collaboration, *PoS* **ICRC2021** (2021) 1053.

[15] **IceCube** Collaboration, *PoS* **ICRC2021** (2021) 1054.

[16] **IceCube** Collaboration, S. Yu, *Moriond EW 2023*, arXiv:2305.16514.

[17] **IceCube** Collaboration, *Phys. Rev. Lett.* **120** (2018), no. 7 071801.

[18] **IceCube** Collaboration, *Phys. Rev. D* **99** (2019), no. 3 032007.

[19] **Super-Kamiokande** Collaboration, *PoS* **ICHEP2020** (2021) 181.

[20] **IceCube** Collaboration, *PoS* **ICRC2019** (2021) 1031.

[21] **IceCube** Collaboration, *PoS* **ICRC2023** (2023) 1036.

PoS(EPS-HEP2023)179